Journal of Photochemistry and Photobiology A: Chemistry 205 (2009) 23–27

Contents lists available at ScienceDirect

Journal of Photochemistry and Photobiology A: Chemistry

journal homepage: www.elsevier.com/locate/jphotochem

Layer-by-layer TiO_2 films as efficient blocking layers in dye-sensitized solar cells

A.O.T. Patrocínio, L.G. Paterno, N.Y. Murakami Iha*

Laboratory of Photochemistry and Energy Conversion, Instituto de Química, Universidade de São Paulo, Av. Prof. Lineu Prestes, 748, 05508-900, São Paulo, Brazil

ARTICLE INFO

Article history:
Received 22 December 2008
Received in revised form 2 April 2009
Accepted 9 April 2009
Available online 19 April 2009

Keywords:
Dye-sensitized solar cell
Blocking layer
TiO_2
Metal oxide layer-by-layer film

ABSTRACT

Charge recombination at the conductor substrate/electrolyte interface has been prevented by using efficient blocking layers of TiO_2 compact films in dye-sensitized solar cell photoanodes. Compact blocking layers have been deposited before the mesoporous TiO_2 film by the layer-by-layer technique using titania nanoparticles as cations and sodium sulfonated polystyrene, PSS, as a polyanion. The TiO_2/PSS blocking layer in a DSC prevents the physical contact of FTO and the electrolyte and leads to a 28% increase in the cell's overall conversion efficiency, from 5.7% to 7.3%.

1. Introduction

Dye-sensitized solar cells, DSCs, have been recognized for their high efficiency on converting light into electricity by using readily available and environmentally friendly materials [1–5]. As a new photovoltaic technology, they hold a promise for large scale solar energy conversion with relatively lower production costs [6–8]. DSCs based on TiO_2 mesoporous photoanodes sensitized by Ru(II) polypyridine complexes have achieved solar energy conversion efficiencies beyond 10% [9–11]. Despite that, an understanding of the limiting factors in the DSC performance is crucial to develop systems with higher efficiencies, stability and lifetime [7,12–14].

Charge recombination is a common process in DSCs that limits their performance [15–17]. It takes place mainly at the TiO_2/sensitizer and FTO/TiO_2 interfaces. According to the kinetic features of the interfacial charge-transfer processes in DSCs [18], charge recombination at the TiO_2/sensitizer interface is negligible. Nevertheless, such a recombination can be further minimized by applying core-shell structured electrodes [19], surface silanization, using co-adsorbents or coating the TiO_2 surface with $TiCl_4$, previously to the sensitizer adsorption [20,21].

At the FTO/TiO_2 interface, charge recombination occurs due to the physical contact between the electrolyte and the FTO surface. The mesoporous structure of the TiO_2 layer allows the percolation of the electrolyte and the electron transfer on the FTO surface becomes feasible. A way to prevent that consists in applying a compact oxide layer on the FTO before the semiconductor mesoporous layer [22,23]. This so-called blocking layer physically blocks the reaction of the photoinjected electrons and the I_3^- ions at the FTO/electrolyte interface.

In solid DSCs with hole-transport materials, blocking layers are essential to avoid the cell's short-circuit [24]. In liquid electrolyte based solar cells, the role of the blocking layer is still under debate, but recent studies have shown an improvement on the cell's efficiency after the use of blocking layers [25–30].

Blocking layers of Nb_2O_5 [28,29,31] and TiO_2 [25,32], have been deposited by different methods such as spray pyrolysis, dip-coating, spin-coating and chemical vapor deposition [30,31,33]. In this contribution, metal oxide layer-by-layer (LbL) films are used as effective blocking layers in DSCs. For this purpose, TiO_2 nanoparticles in acidic pH and sodium sulfonated polystyrene were used as cationic and anionic species respectively and the resulting LbL film has been spectroscopically and morphologically characterized before photoeletrochemical experiments to evaluate its effectiveness.

2. Experimental

All chemicals, analytical or HPLC grade, were used as received, with the exception of 3-methyl-2-oxazolidinone (Aldrich), which was purified by distillation under reduced pressure. The N3 dye, *cis*-$[Ru(dcbH_2)_2(NCS)_2]$, $dcbH_2$ = 4,4′-dicarboxylic acid-2,2′-bipyridine, was synthesized as previously reported [34].

TiO_2 nanoparticles were prepared by the sol–gel method according to procedures reported elsewhere [34,35]. 24 mL of titanium(IV) isoproxide (Strem, 98%) were slowly added to 140 mL of 0.1 mol L^{-1} HNO_3 aqueous solution under vigorous stirring. The mixture was left under stirring and heated (80 °C) for 8 h. TiO_2 particles of 5–10 nm in diameter, as determined by STEM microscopy, were pro-

* Corresponding author. Tel.: +55 11 3091 2151; fax: +55 11 3815 5579.
E-mail address: neydeiha@iq.usp.br (N.Y. Murakami Iha).

1010-6030/$ – see front matter © 2009 Elsevier B.V. All rights reserved.
doi:10.1016/j.jphotochem.2009.04.008

duced. An aliquot of the sol was separated for the blocking layer deposition. The remaining aliquot was autoclaved for 8 h at 200 °C in a titanium pressure vessel to increase particles' size to 20–30 nm. The autoclaved sol was then concentrated to ~180 mg mL^{-1} and stabilized with Carbowax 20 M (Supelco) to produce a paste for the deposition of the mesoporous layer.

TiO_2 compact films used as blocking layers were deposited onto cleaned FTO substrates (Pilkington TEC–15, 15 Ω □$^{-1}$) using the LbL technique, following a similar procedure reported in the literature [36]. The substrate was immersed alternately for 5 min in a 10 mg mL^{-1} suspension of the non-autoclaved TiO_2 sol at pH 2 and in an 1.0 mg mL^{-1} sodium sulfonated polystyrene, PSS, (Aldrich; M_W = 70,000 g mol^{-1}) aqueous solution at pH 5. After each immersion, the films were rinsed with reagent-grade water (30 s, under magnetic stirring) and dried with compressed air. In this approach, TiO_2 nanoparticles were used as cations and PSS as a polyanion.

The mesoporous TiO_2 layer (~6 μm thickness) was deposited by painting onto either the bare FTO substrates or those containing the compact TiO_2/PSS blocking layer. The film was dried at room temperature and sintered at 450 °C for 30 min. The sensitization was achieved by immersion of electrodes in a N3 saturated ethanolic solution. The cell, with 0.25 cm^2 active area, was assembled in a sandwich-type arrangement using the sensitized TiO_2 photoanode and a transparent Pt-covered FTO (Pilkington, TEC-15) as a counter-electrode. A solution of 0.03 mol L^{-1} I_2/0.3 mol L^{-1} LiI/0.5 mol L^{-1} pyridine in 90:10 mixture of acetonitrile (Aldrich) and 3-methyl-2-oxazolidinone was used as an electrolyte mediator.

Three different types of photoanodes were prepared to evaluate the effectiveness of the TiO_2/PSS films as blocking layers: mesoTiO_2, a reference in which only the mesoporous TiO_2 layer has been deposited on a FTO substrate, TiO_2/PSS-mesoTiO_2, which contains the TiO_2/PSS film onto FTO before the TiO_2 mesoporous layer and $TiCl_4$-mesoTiO_2, in which the FTO substrate was treated with a $TiCl_4$ solution before deposition of the mesoporous TiO_2 layer, as described in the literature [37].

UV–vis absorption spectra were obtained by using an 8453 UV–vis spectrophotometer (Hewlett Packard). The size of TiO_2 nanoparticles and the morphology of the films were evaluated by scanning transmission electron microscopy (STEM) and field-emission scanning electron microscopy (FESEM) using a JSM 7401F (JEOL) microscope. The film thicknesses were measured with an Alpha step (KLA Tencor) perfilometer. Thermogravimetric analysis was conducted in air by using a TGA 50 (Shimadzu) thermoanalyser.

Photoelectrochemical characterization of DSC was carried out by current-potential measurements using a PAR270 galvanostat/potentiostat (EG&G Instruments) system at simulated AM 1.5 solar radiation (78 mW cm^{-2}) provided by a solar simulator (Newport/Oriel) as previously described [35,38]. All parameters were determined from the average values measured with at least five individual cells of each type of photoanode.

3. Results and discussion

The deposition of the TiO_2/PSS bilayers on a quartz slide was monitored by UV–vis spectroscopy, Fig. 1. A linear increase on the absorbance at 270 nm can be observed as the number of TiO_2/PSS bilayers increases (Fig. 1, insert), due to a same amount of PSS being adsorbed in each deposition cycle. Since the films are assembled via electrostatic interactions, the amount of TiO_2 nanoparticles should also be constant at each deposition to compensate the negative charges of PSS and allow the regular stepwise growth of the films. Similar observations were made by He et al. [39] using different types of polyelectrolytes.

The transmittance spectra of both substrates, bare FTO and those containing a TiO_2/PSS film, are presented in Fig. 2. In the visible

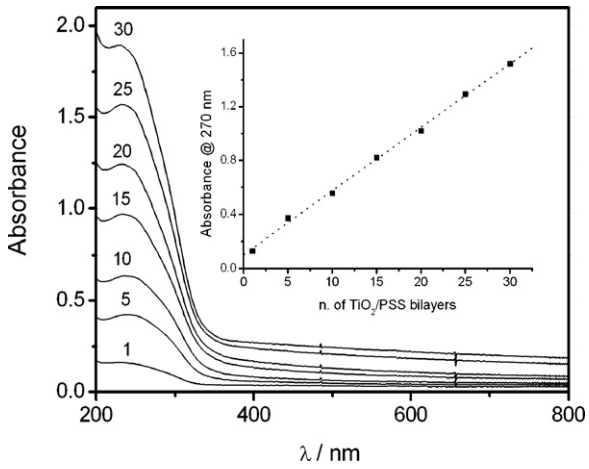

Fig. 1. UV–vis absorption spectra of TiO_2/PSS LbL films on quartz slide with 1, 5, 10, 15, 20, 25, and 30 bilayers. The insert shows the absorbance increase at 270 nm with the number of bilayers.

region, transmittance of the bare FTO decreased from 80% to 60% after deposition of 30 TiO_2/PSS bilayers. A similar decrease observed by Yu et al. [40] for optical fibers coated with 24 TiO_2/PSS bilayers was attributed to the light reflection produced by the oxide nanoparticles. On the other hand, the $TiCl_4$ treatment did not significantly change the substrate transmittance since a very thin layer was obtained.

The morphology of the mesoporous TiO_2 and the TiO_2/PSS films was evaluated by FESEM micrographs, Fig. 3. Unlike the mesoporous TiO_2 film, Fig. 3a, the TiO_2/PSS film, Fig. 3b, is compact, with plates of nanoparticles aggregates. We have attributed this unusual morphology to the reduced size of the TiO_2 nanoparticles and the presence of the PSS chains. These small nanoparticles can be more efficiently packed onto the substrate surface, since voids among particles are reduced as their size decreases. As the bilayers are being deposited, layers of TiO_2 nanoparticles stack onto each other, preferably on the voids left by the previous layer. Thus, nanoparticles of adjacent layers are in close contact and the result is a densely packed film. Meanwhile, the adsorbed PSS chains act as a "glue" to hold the nanoparticles together within the film and to minimize electrostatic repulsions.

It is reasonable to assume that a major part of PSS is still within the film after its sinterization, as it was not detected any visible changes on the morphology of the TiO_2/PSS film after sintering

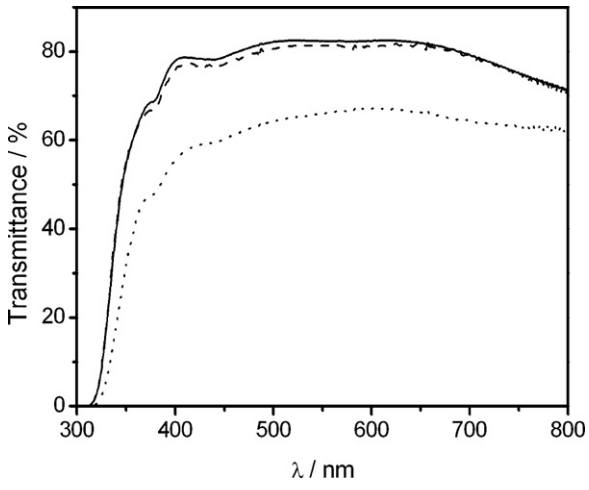

Fig. 2. Transmittance spectra of bare FTO substrate (—), after $TiCl_4$ treatment (- - - -) or after 30 bilayers deposition of TiO_2/PSS (. . .).

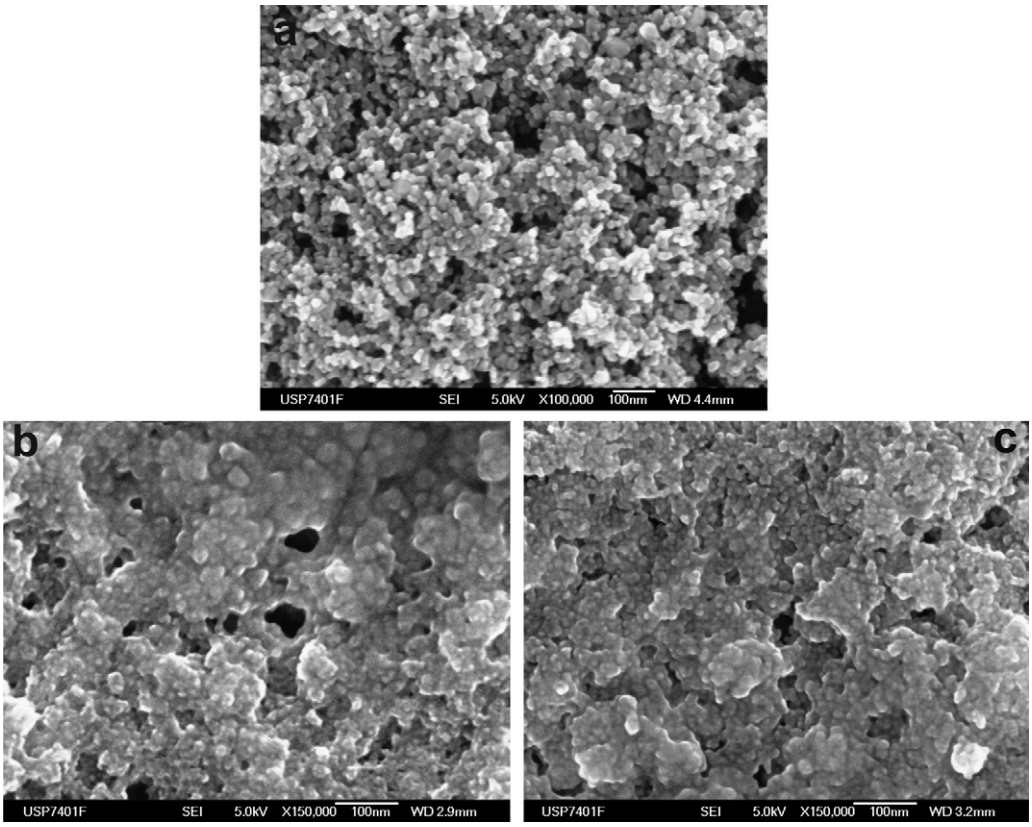

Fig. 3. FESEM micrographs of the mesoporous TiO_2 layer (a), TiO_2/PSS film, 30 bilayers, before (b) and after (c) sintering.

at 450 °C, Fig. 3c, and the thermogravimetric analyses of the PSS employed shows that only 18% of the mass is lost at 500 °C.

The surface concentration of the N3 dye ($\sim 1 \times 10^{-7}$ mol cm^{-2}) was identical, within the experimental error, on the mesoporous TiO_2 film of the three types of photoanodes investigated. Thus, the dye adsorption preferably occurred onto the mesoporous TiO_2 layer and was practically negligible onto the blocking layers.

LbL TiO_2 films have been already employed in DSCs, although with different approaches. He et al. [39] used them as mesoporous layer and, more recently, Agrios et al. [41] as mesoporous and scattering layers.

The dark current–voltage characteristics of DSC for different types of TiO_2 photoanodes are shown in Fig. 4. It is noteworthy to see that the blocking layers increase the open-circuit voltage, V_{oc}. The highest V_{oc} under dark conditions is for the DSC having the TiO_2/PSS film (30 bilayers), which indicates the effectiveness of such a film as a blocking layer due to inhibition of the electron recombination in the FTO/electrolyte interface.

Under illumination, Fig. 5, the solar cell with the TiO_2/PSS-mesoTiO_2 photoanode provided the highest photocurrent among the other cells. Photoelectrochemical parameters determined for DSCs with different photoanodes are listed in the Table 1.

A slight increase, ~50 mV, on the cells' V_{oc} can be observed when $TiCl_4$ or TiO_2/PSS blocking layers were employed. J_{sc} was also higher for those devices, approximately 6.8% and 19%, respectively, for solar cells with $TiCl_4$-mesoTiO_2 and TiO_2/PSS-mesoTiO_2 photoanodes. The cell's overall efficiency increased 28% going from 5.7% to 7.3% with the use of TiO_2/PSS-mesoTiO_2 photoanodes.

These results are in accordance with theoretical studies [42,43] that predict an increase on both J_{sc} and V_{oc} when the recombination rate at the FTO/electrolyte interface decreases. Experimental results reported by Cameron and co-workers [25,26,44] attained with DSC having TiO_2 films deposited by spray pyrolysis as blocking layers confirmed such a prediction and corroborated the results presented here.

Table 1
Photoelectrochemical parameters of DSCs with different photoanodes (AM 1.5 solar radiation; P_{irr} = 78 mW cm^{-2}).

Photoanode	V_{oc}/V	J_{sc}/mA cm^{-2}	ff	η/%
MesoTiO_2	0.68 ± 0.02	10.2 ± 0.5	0.64 ± 0.03	5.7 ± 0.3
$TiCl_4$-mesoTiO_2	0.70 ± 0.02	10.9 ± 0.5	0.64 ± 0.03	6.5 ± 0.3
TiO_2/PSS-mesoTiO_2	0.73 ± 0.01	12.6 ± 0.5	0.62 ± 0.03	7.3 ± 0.3

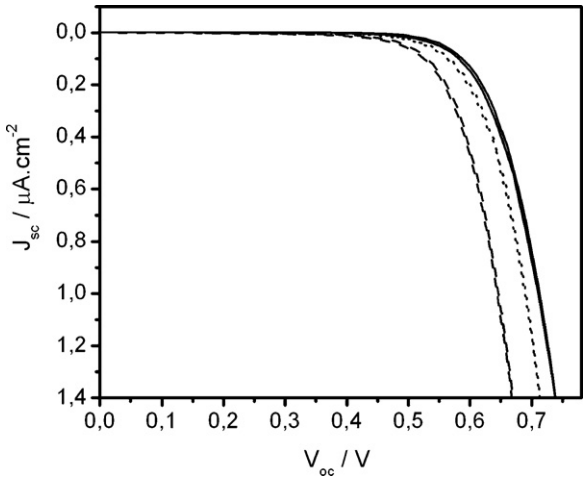

Fig. 4. Dark current–voltage curves of DSC with different photoanodes: TiO_2/PSS-mesoTiO_2 (—), mesoTiO_2 (- - - -) and $TiCl_4$-mesoTiO_2 (. . .).

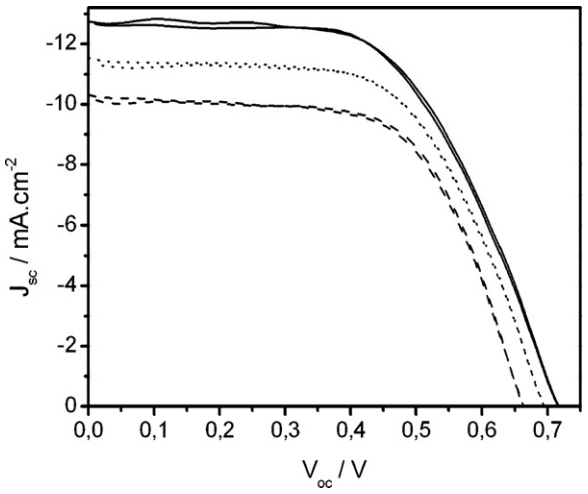

Fig. 5. Current–voltage curves under illumination (AM 1.5; 78 mW cm^{-2}) of DSCs with different photoanodes: TiO_2/PSS-mesoTiO_2 (—), mesoTiO_2 (----) and $TiCl_4$-mesoTiO_2 (. . .).

It can be inferred that the TiO_2/PSS film is a more effective blocking layer than the $TiCl_4$ film due to its morphology and thickness. The compact film with reduced porosity acts as an efficient blocking layer capable to prevent the physical contact of the I_3^- anions to the FTO surface. Further studies to determine the role of the blocking layer thickness and the influence of the PSS residues on their effectiveness are in progress.

4. Conclusions

TiO_2/PSS films deposited via LbL technique were successfully used as blocking layers in dye-sensitized solar cells based on liquid electrolytes, due to their compact structure. This avoided direct contact between the FTO substrate and electrolyte and prevented the electron recombination. As a consequence, higher V_{oc} and J_{sc} values were achieved and the overall cell's efficiency was improved 28%. This result has proven the importance of the compact oxide blocking layer in liquid based DSC to control the charge recombination processes [45].

Acknowledgments

We thank the Fundação de Amparo à Pesquisa do Estado de São Paulo (FAPESP) and the Conselho Nacional de Desenvolvimento Científico e Tecnológico (CNPq) for the financial support and Pilkington Glass Company for supplying FTO glasses.

References

[1] J.M. Kroon, N.J. Bakker, H.J.P. Smit, P. Liska, K.R. Thampi, P. Wang, S.M. Zakeeruddin, M. Grätzel, A. Hinsch, S. Hore, U. Wurfel, R. Sastrawan, J.R. Durrant, E. Palomares, H. Pettersson, T. Gruszecki, J. Walter, K. Skupien, G.E. Tulloch, Nanocrystalline dye-sensitized solar cells having maximum performance, Prog. Photovolt. 15 (2007) 1–18.
[2] M. Grätzel, Dye-sensitized solar cells, J. Phtochem. Photobiol. C: Photochem. Rev. 4 (2003) 145–153.
[3] M. Grätzel, Photoelectrochemical cells, Nature 414 (2001) 338–344.
[4] S. Yanagida, Recent research progress of dye-sensitized solar cells in Japan, C. R. Chim. 9 (2006) 597–604.
[5] S. Anandan, Recent improvements and arising challenges in dye-sensitized solar cells, Sol. Energy Mater. Sol. Cells 91 (2007) 843–846.
[6] A.S. Polo, M.K. Itokazu, N.Y.M. Iha, Metal complex sensitizers in dye-sensitized solar cells, Coord. Chem. Rev. 248 (2004) 1343–1361.
[7] C.G. Garcia, J.F. de Lima, N.Y. Murakami Iha, Energy conversion: from the ligand field photochemistry to solar cells, Coord. Chem. Rev. 196 (2000) 219–247.
[8] M.D. Wei, Y. Konishi, H.S. Zhou, M. Yanagida, H. Sugihara, H. Arakawa, Highly efficient dye-sensitized solar cells composed of mesoporous titanium dioxide, J. Mater. Chem. 16 (2006) 1287–1293.
[9] Y. Chiba, A. Islam, R. Komiya, N. Koide, L.Y. Han, Conversion efficiency of 10.8% by a dye-sensitized solar cell using a TiO_2 electrode with high haze, Appl. Phys. Lett. 88 (2006) 223505.
[10] Y. Chiba, A. Islam, Y. Watanabe, R. Komiya, N. Koide, L.Y. Han, Dye-sensitized solar cells with conversion efficiency of 11.1%, Jpn. J. Appl. Phys. 45 (2) (2006) L638–L640.
[11] S. Ito, T.N. Murakami, P. Comte, P. Liska, C. Grätzel, M.K. Nazeeruddin, M. Grätzel, Fabrication of thin film dye-sensitized solar cells with solar to electric power conversion efficiency over 10%, Thin Solid Films 516 (2008) 4613–4619.
[12] B.A. Gregg, F. Pichot, S. Ferrere, C.L. Fields, Interfacial recombination processes in dye-sensitized solar cells and methods to passivate the interfaces, J. Phys. Chem. B 105 (2001) 1422–1429.
[13] C.G. Garcia, A.K. Nakano, C.J. Kleverlaan, N.Y. Murakami Iha, Electron injection versus charge recombination in photoelectrochemical solar cells using *cis*-$[(dcbH_2)_2Ru(CNpy)(H_2O)]Cl^{-2}$ as a nanocrystalline TiO_2 sensitizer, J. Photochem. Photobiol. A: Chem. 151 (2002) 165–170.
[14] C.G. Garcia, C.J. Kleverlaan, C.A. Bignozzi, N.Y. Murakami Iha, Time-resolved experiments in dye-sensitized solar cells using $[(dcbH_2)_2Ru(ppy)_2](ClO_4)_2$ as a nanocrystalline TiO_2 sensitizer, J. Photochem. Photobiol. A: Chem. 147 (2002) 143–148.
[15] A.N.M. Green, E. Palomares, S.A. Haque, J.M. Kroon, J.R. Durrant, Charge transport versus recombination in dye-sensitized solar cells employing nanocrystalline TiO_2 and SnO_2 films, J. Phys. Chem. B 109 (2005) 12525–12533.
[16] S.A. Haque, E. Palomares, B.M. Cho, A.N.M. Green, N. Hirata, D.R. Klug, J.R. Durrant, Charge separation versus recombination in dye-sensitized nanocrystalline solar cells: the minimization of kinetic redundancy, J. Am. Chem. Soc. 127 (2005) 3456–3462.
[17] M. Ni, M.K.H. Leung, D.Y.C. Leung, K. Sumathy, Theoretical modeling of TiO_2/TCO interfacial effect on dye-sensitized solar cell performance, Sol. Energy Mater. Sol. Cells 90 (2006) 2000–2009.
[18] M. Grätzel, Solar energy conversion by dye-sensitized photovoltaic cells, Inorg. Chem. 44 (2005) 6841–6851.
[19] Y. Diamant, S. Chappel, S.G. Chen, O. Melamed, A. Zaban, Core-shell nanoporous electrode for dye-sensitized solar cells: the effect of shell characteristics on the electronic properties of the electrode, Coord. Chem. Rev. 248 (2004) 1271–1276.
[20] B.C. O'Regan, J.R. Durrant, P.M. Sommeling, N.J. Bakker, Influence of the $TiCl_4$ treatment on nanocrystalline TiO_2 films in dye-sensitized solar cells. 2. Charge density, band edge shifts, and quantification of recombination losses at short circuit, J. Phys. Chem. C 111 (2007) 14001–14010.
[21] P.M. Sommeling, B.C. O'Regan, R.R. Haswell, H.J.P. Smit, N.J. Bakker, J.J.T. Smits, J.M. Kroon, J.A.M. van Roosmalen, Influence of a $TiCl_4$ post-treatment on nanocrystalline TiO_2 films in dye-sensitized solar cells, J. Phys. Chem. B 110 (2006) 19191–19197.
[22] B. Peng, G. Jungmann, C. Jager, D. Haarer, H.W. Schmidt, M. Thelakkat, Systematic investigation of the role of compact TiO_2 layer in solid state dye-sensitized TiO_2 solar cells, Coord. Chem. Rev. 248 (2004) 1479–1489.
[23] E. Palomares, J.N. Clifford, S.A. Haque, T. Lutz, J.R. Durrant, Control of charge recombination dynamics in dye-sensitized solar cells by the use of conformally deposited metal oxide blocking layers, J. Am. Chem. Soc. 125 (2003) 475–482.
[24] C.S. Karthikeyan, K. Peter, H. Wietasch, M. Thelakkat, Highly efficient solid-state dye-sensitized TiO_2 solar cells via control of retardation of recombination using novel donor-antenna dyes, Sol. Energy Mater. Sol. Cells 91 (2007) 432–439.
[25] P.J. Cameron, L.M. Peter, Characterization of titanium dioxide blocking layers in dye-sensitized nanocrystalline solar cells, J. Phys. Chem. B 107 (2003) 14394–14400.
[26] P.J. Cameron, L.M. Peter, S. Hore, How important is the back reaction of electrons via the substrate in dye-sensitized nanocrystalline solar cells? J. Phys. Chem. B 109 (2005) 930–936.
[27] A. Burke, S. Ito, H. Snaith, U. Bach, J. Kwiatkowski, M. Grätzel, The function of a TiO_2 compact layer in dye-sensitized solar cells incorporating "Planar" organic dyes, Nano Lett. 8 (2008) 977–981.
[28] J.B. Xia, N. Masaki, K.J. Jiang, S. Yanagida, Sputtered, Nb_2O_5 as a novel blocking layer at conducting Glass/TiO_2 interfaces in dye-sensitized ionic liquid solar cells, J. Phys. Chem. C 111 (2007) 8092–8097.
[29] J.B. Xia, N. Masaki, K.J. Jiang, S. Yanagida, Sputtered, Nb_2O_5 as an effective blocking layer at conducting glass and TiO_2 interfaces in ionic liquid-based dye-sensitized solar cells, Chem. Commun. (2007) 138–140.
[30] J. Xia, N. Masaki, K. Jiang, S. Yanagida, Deposition of a thin film of TiOx from a titanium metal target as novel blocking layers at conducting glass/TiO_2 interfaces in ionic liquid mesoscopic TiO_2 dye-sensitized solar cells, J. Phys. Chem. B 110 (2006) 25222–25228.
[31] J.B. Xia, N. Masaki, K.J. Jiang, S. Yanagida, Fabrication and characterization of thin Nb_2O_5 blocking layers for ionic liquid-based dye-sensitized solar cells, J. Photochem. Photobiol. A: Chem. 188 (2007) 120–127.
[32] L.H. Hu, S.Y. Dai, J. Weng, S.F. Xiao, Y.F. Sui, Y. Huang, S.H. Chen, F.T. Kong, X. Pan, L.Y. Liang, K.J. Wang, Microstructure design of nanoporous TiO_2 photoelectrodes for dye-sensitized solar cell modules, J. Phys. Chem. B 111 (2007) 358–362.
[33] H. Goto, R. Hattori, High temperature sputtered TiO_2 film as an efficient blocking layer for the dye-sensitized solar cells, Electrochemistry 74 (2006) 484–486.
[34] M.K. Nazeeruddin, A. Kay, I. Rodicio, R. Humphrybaker, E. Muller, P. Liska, N. Vlachopoulos, M. Grätzel, Conversion of Light to Electricity by *cis*-X_2bis(2,2′-Bipyridyl-4,4′-Dicarboxylate)Ruthenium(II) Charge-Transfer Sensitizers (X = Cl^-, Br^-, I^-, Cn^-, and SCN^-) on Nanocrystalline TiO_2 Electrodes, J. Am. Chem. Soc. 115 (1993) 6382–6390.

[35] A.O.T. Patrocínio, E.B. Paniago, R.M. Paniago, N.Y.M. Iha, XPS characterization of sensitized *n*-TiO_2 thin films for dye-sensitized solar cell applications, Appl. Surf. Sci. 254 (2008) 1874–1879.
[36] L.G. Paterno, L.H.C. Mattoso, Effect of pH on the preparation of self-assembled films of poly(*o*-ethoxyaniline) and sulfonated lignin, Polymer 42 (2001) 5239–5245.
[37] P. Wang, S.M. Zakeeruddin, J.E. Moser, M. Grätzel, A new ionic liquid electrolyte enhances the conversion efficiency of dye-sensitized solar cells, J. Phys. Chem. B 107 (2003) 13280–13285.
[38] A.S. Polo, N.Y.M. Iha, Blue sensitizers for solar cells: Natural dyes from Calafate and Jaboticaba, Sol. Energy Mater. Sol. Cells 90 (2006) 1936–1944.
[39] J.A. He, R. Mosurkal, L.A. Samuelson, L. Li, J. Kumar, Dye-sensitized solar cell fabricated by electrostatic layer-by-layer assembly of amphoteric TiO_2 nanoparticles, Langmuir 19 (2003) 2169–2174.
[40] H.H. Yu, D.S. Jiang, X.F. Li, D.S. Yu, L.D. Zhou, Layer-by-layer assembly of polyelectrolyte/TiO_2 thin films with reflection-enhancing function, Opt. Mater. 28 (2006) 1381–1384.
[41] A.G. Agrios, I. Cesar, P. Comte, M.K. Nazeeruddin, M. Grätzel, Nanostructured composite films for dye-sensitized solar cells by electrostatic layer-by-layer deposition, Chem. Mater. 18 (2006) 5395–5397.
[42] J. Ferber, R. Stangl, J. Luther, An electrical model of the dye-sensitized solar cell, Sol. Energy Mater. Sol. Cells 53 (1998) 29–54.
[43] L. Peter, Transport, trapping and interfacial transfer of electrons in dye-sensitized nanocrystalline solar cells, J. Electroanal. Chem. 599 (2007) 233–240.
[44] P.J. Cameron, L.M. Peter, How does back-reaction at the conducting glass substrate influence the dynamic photovoltage response of nanocrystalline dye-sensitized solar cells? J. Phys. Chem. B 109 (2005) 7392–7398.
[45] Patent INPI/SP on 14/08/08, P. I. 0.802.589-4.